Science Bulletin 64 (2019) 964–967

Contents lists available at ScienceDirect

Science Bulletin

journal homepage: www.elsevier.com/locate/scib

Short Communication

Multistep evolution from a metal–organic framework to ultrathin nanosheets

Yun Li[a], Jin Huang[a], Zong-Wen Mo[a], Xue-Wen Zhang[a], Xiao-Ning Cheng[b], Li Gong[b], Dong-Dong Zhou[a,*], Jie-Peng Zhang[a,*]

[a] MOE Key Laboratory of Bioinorganic and Synthetic Chemistry, School of Chemistry, Sun Yat-Sen University, Guangzhou 510275, China
[b] Instrumental Analysis and Research Center, Sun Yat-Sen University, Guangzhou 510275, China

ARTICLE INFO

Article history:
Received 2 April 2019
Received in revised form 8 May 2019
Accepted 10 May 2019
Available online 16 May 2019

Two-dimensional (2D) materials and ultrathin nanosheets have attracted tremendous research interests [1–4]. Exfoliation of porous coordination polymers (PCPs) or metal–organic frameworks (MOFs) with 2D coordination structures is emerging as a viable strategy for preparation of new types of 2D materials [5–8]. The relatively weak bonding within and strong interactions between 2D coordination networks are the main problems for successful exfoliation [9]. Pretreatments of the layered MOFs to expand the interlayer distances can be helpful [10–12]. Capturing the exfoliation intermediates and visualizing their structures are valuable for understanding the exfoliation mechanism and confirming the structures of the final 2D materials [11,12].

While crystal-to-crystal and single-crystal-to-single-crystal structural transformations of MOFs have been widely reported, those involving reconstitution of coordination bonds and topologies (e.g., from 3D to 2D) are rare, because the tension and shearing forces tend to degrade crystallinity, especially single-crystallinity [13–17]. Two examples reported single-crystal structures of the intermediate states of MOF exfoliation [11,12]. Jiang group and Zhou group [11] treated a MOF crystal with 2D coordination structure by 4,4′-dipyridyl disulfide to expand the interlayer distance, and then exfoliated the latter by trimethylphosphine. Single-crystal structure showed that the 4,4′-dipyridyl disulfide served as a terminal rather than bridging ligand. Aida group [12] showed that a MOF crystal with 2D coordination network can be exfoliated in different solvents to form ultrathin nanosheets with thickness of either 1.3 or 2.0 nm. Single-crystal structures of the intermediates showed that the disordered solvent molecules inserted between monolayers and bilayers, explaining the different thicknesses of the products. Recently, we showed that pillared-layer MOFs may be good candidates for preparation of 2D materials, by virtue of selective breaking the pillar ligands [18]. Here, we report a new pillared-layer MOF which can be easily exfoliated to form ultrathin nanosheets with multiple single-crystalline or polycrystalline intermediate states.

Solvothermal reaction of $Cd(NO_3)_2{\cdot}4H_2O$ with 2,3-dihydroxy-1,4-benzenedicarboxylic acid (H_4dhbdc) in mixed solvent containing *N*,*N*-dimethylformamide (DMF) and H_2O afforded crystals of $(H_3O)_2[Cd_4(\mathrm{dhbdc})_2(H_2\mathrm{dhbdc})(\mathrm{DMF})_4]{\cdot}H_2O$ (**1**) crystallizing in the *C*2/*c* space group (Table S1 online), which has a 3D anionic pillared-layer structure consisting of neutral wavelike $\{Cd_2(\mathrm{dhbdc})\}$ layers running across the *bc*-plane (Fig. 1) and anionic $H_2\mathrm{dhbdc}^{2-}$ pillars (Fig. 2a). In the $\{Cd_2(\mathrm{dhbdc})\}$ layer, each dhbdc^{4-} coordinates with 6 Cd^{2+} ions with 9 coordination bonds (3 pairs are bidentate chelating) and each Cd^{2+} ion coordinates with 4 or 5 oxygen atoms from three dhbdc^{4-} ligands (Fig. S1 online). The vacant coordination sites of Cd^{2+} are capped by one oxygen atom from DMF and one carboxylate oxygen atom of the $H_2\mathrm{dhbdc}^{2-}$ pillars at opposite sides of the layer to furnish the octahedron or decahedron coordination geometry (Fig. S1 online). The 3D pillared-layer structure has an interlayer separation of 10.2 Å and a pillar inclining angle of 79.7° (Figs. 2a and S2 (online)). There are 2D intersecting channels between the layers, which are occupied by the H_3O^+/H_2O guests. Thermogravimertry and powder X-ray diffraction (PXRD) showed that after removal of the guest and coordinated solvent molecules (Fig. S3 online), the host of **1** loses crystallinity (Fig. S4 online).

In water, **1** quickly transforms to a new structure $[Cd_4(\mathrm{dhbdc})_2(H_2O)_8]{\cdot}2H_2O{\cdot}H_4\mathrm{dhbdc}$ (**4**) as microcrystals (Fig. S5 online). Further, $(H_3O)_2[Cd_4(\mathrm{dhbdc})_2(H_2\mathrm{dhbdc})(H_2O)_4]{\cdot}H_2O$ (**2**) and $(H_3O)[Cd_4(\mathrm{dhbdc})_2(H_3\mathrm{dhbdc})(H_2O)_7]{\cdot}2H_2O$ (**3**) were captured as single-crystalline intermediates between **1** and **4**, by using

---

* Corresponding authors.

E-mail addresses: zhoudd3@mail.sysu.edu.cn (D.-D. Zhou), zhangjp7@mail.sysu.edu.cn (J.-P. Zhang).

https://doi.org/10.1016/j.scib.2019.05.011
2095-9273/

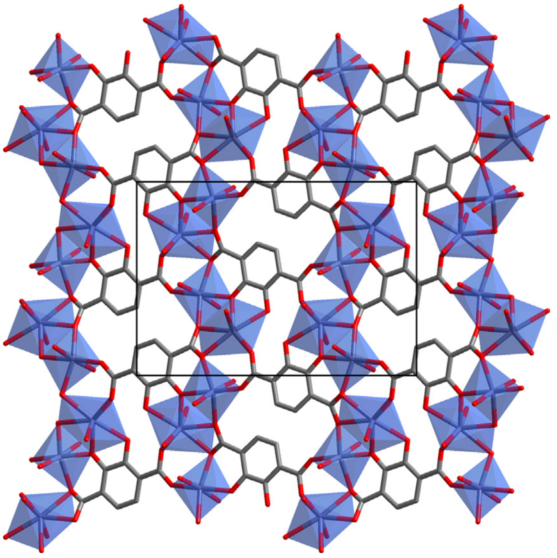

Fig. 1. (Color online) The $\{Cd_2(dhbdc)\}$ layer in **1**. The coordinated oxygen atoms from DMF and H_2dhbdc^{2-} are added to show the coordination geometries of the metal ions as semi-transparent polyhedra.

milder reaction conditions, i.e., immersing **1** in methanol (containing ca. 0.05 wt% H_2O) and exposing **2** in H_2O vapor, respectively (Figs. S6–S8 online). **2** and **3** can also transform to **4** in water (Fig. S9 online), and **2**–**4** can all transform back to **1** in DMF vapor (Fig. S10 online).

2 and **3** both crystallize in the same space group as **1** (Table S1 online). The *b*- and *c*-axes of **2** and **3** change less than 3% from those of **1**, indicating that the $\{Cd_2(dhbdc)\}$ layers are kept with little distortion (Figs. S11 and S12 online). In contrast, the *a*-axis significantly shrinks from 24.0 Å for **1** to 17.3 Å for **2** and further to 16.0 Å for **3**, corresponding to the reduction of the interlayer separation from 10.2 Å for **1** to 8.4 Å for **2** (Fig. 2b) and further to 7.6 Å for **3** (Fig. 2c). Also, β reduces from 122.1° for **1** to 105.0° for **2** and 108.7° for **3** (Table S1 online), indicating the change of inclining angle of the pillars and sliding between adjacent $\{Cd_2(dhbdc)\}$ layers. Structural refinements of the single-crystal structures showed that the metal ions and organic ligands in **2** have the same coordination modes as for **1**, except that the coordinated DMF molecules are replaced by H_2O molecules (Fig. S1 online). **2** retains the 3D anionic pillared-layer structure, but the pillar inclining angle significantly reduces from 79.7° to 45.2° (Fig. S2 online), accounting for the reduction of interlayer distance, which can be explained by the very different molecular sizes of the coordinated DMF and H_2O molecules.

In **3**, the coordination modes of metal ions and $dhbdc^{4-}$, as well as $\{Cd_2(dhbdc)\}$ layers were retained (Figs. S1, S11 and S12 online). However, **3** turned into a 2D coordination structure (Fig. 2c). Each H_2dhbdc^{2-} pillar in **1** and **2** uses its two carboxylate groups to coordinate two pairs of Cd^{2+} ions from two layers, but in **3** each H_3dhbdc^{-} "pillar" uses only one carboxylate group in the monodentate mode to coordinate with one Cd^{2+} (Fig. S1 online). In other words, one bidentate anchoring end of H_2dhbdc^{2-} completely leaves the layer (replaced by two H_2O ligands) and simultaneous protonated by the guest H_3O^{+} to form H_3dhbdc^{-}, and another bidentate anchoring end becomes monodentate (replaced by one H_2O ligand). The dangling H_3dhbdc^{-} is almost parallel with the $\{Cd_2(dhbdc)\}$ layer, with an inclining angle of 9.8° (Fig. S3 online).

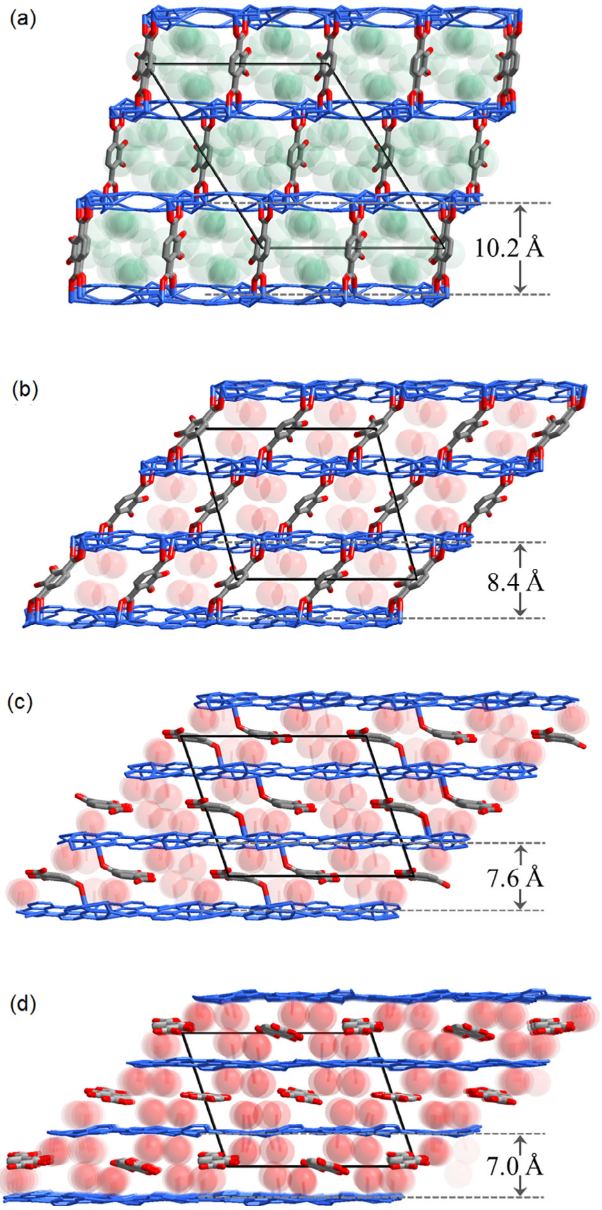

Fig. 2. (Color online) Crystal structures of (a) **1**, (b) **2**, (c) **3**, and (d) **4** viewing along the *b*-axis. For clarity, $\{Cd_2(dhbdc)\}$ layers are drawn in blue, $H_2dhbdc^{2-}/H_3dhbdc^{-}/H_4dhbdc$ pillars are drawn as thick sticks, and coordinated solvent molecules are drawn in the space-filling and semi-transparent mode. Hydrogen atoms, guest water and hydronium are omitted.

Microcrystalline **4** displays weak and simple PXRD pattern, indicating partial loss of long-range order and preventing us to experimentally determine its crystal structure. According to the main diffraction peak of **4** at 12.7°, the interlayer distance can be calculated as 7.0 Å. Considering the situation of the "pillars" as seen in **3**, they may leave the $\{Cd_2(dhbdc)\}$ layers and even the crystals. Infrared (IR) spectra showed that, **4** retains the C–O(H) stretch vibration and CO–H bending vibration (Fig. S13 online), meaning that the "pillars" are still in the crystals. We simulated the crystal structure of **4** (Fig. 2d), by replacing the "pillars" in the crystal structure of **3** with H_2O ligands, setting the interlayer separation to 7.0 Å, optimizing the structure with molecular mechanics, and finally load H_4dhbdc and H_2O guests into the structure by the Grand Canonical Monte Carlo method. If the interlayer separation was set shorter, H_4dhbdc guest molecules cannot be loaded. This further confirmed the presence of H_4dhbdc guest molecules between the layers in **4**, which could help separating the layers or weakening the interlayer interactions for preparation of ultrathin nanosheets [11,12].

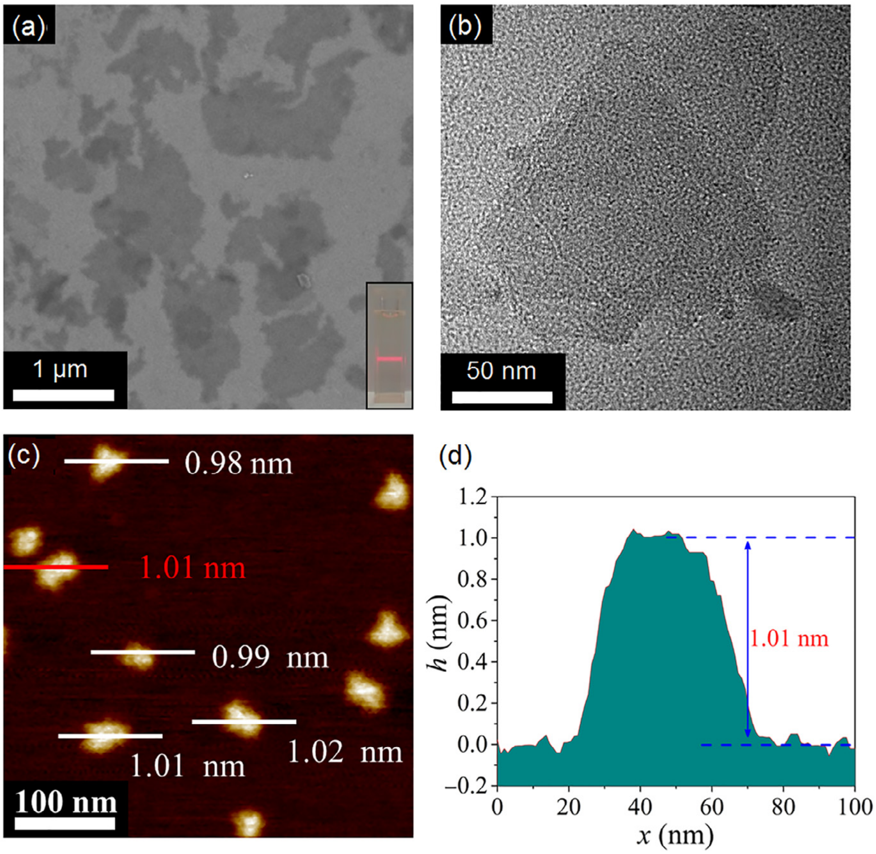

Fig. 3. (Color online) (a) SEM image (inset: an optical image showing the Tyndall effect), (b) TEM image, (c) AFM image with thickness measurements and (d) the corresponding height profile of **NS**.

Indeed, simple sonication of **4** in H_2O produced ultrathin nanosheets of $[Cd_2(dhbdc)(H_2O)_4]$ (**NS**) with no PXRD peak (Fig. S14 online). Replacing **4** by **1** can also give the same result, confirming **4** as an intermediate of the evolution from **1** to **NS** (Fig. S14 online). IR spectra showed that, in **NS** the C–O(H) stretch vibration (1,248 cm^{-1}) and CO–H bending vibration (1,510 cm^{-1}) disappeared (Fig. S13 online), confirming the removal of the “pillars”. Elemental analysis gave a chemical composition consistent with the proposed formula $[Cd_2(dhbdc)(H_2O)_4]$. Scanning electron microscopy (SEM) demonstrated the thin slice morphology (Fig. 3a). Wrinkled or ruptured nanosheets were observed from transmission electron microscopy (TEM) (Fig. 3b). Atomic force microscopy (AFM) gave thickness of ca. 1.0 nm (Fig. 3c and d), corresponding well with the thickness of a single layer of $[Cd_2(dhbdc)(H_2O)_4]$ containing coordination H_2O molecules, which can be simulated from **3** or **4** (Fig. S15 online). It should be noted that, the water dispersion of **NS** can be stable for at least 3 months (Fig. S16 online) [19].

In summary, we synthesized a new pillared-layer MOF which can be easily exfoliated to form ultrathin nanosheets in water. Interestingly, the exfoliation proceeds via multiple steps, and the intermediates can keep good crystallinity and even single-crystallinity, enabling us to directly visualize how water molecules attack the layers and replace the pillars. Similar exfoliation processes may occur in other systems when the layers have sufficiently high stability and the pillar-layer binding strengths are moderate. Preliminary study showed that the Mn analogue of **1** can display similar exfoliation processes.

Conflict of interest

The authors declare that they have no conflict of interest.

Acknowledgments

This work was supported by the National Natural Science Foundation of China (21731007, 21701191, and 21821003), the Guangdong Pearl River Talents Program (2017BT01C161), and the Fundamental Research Funds for the Central Universities (18lgpy42).

Author contributions

Jie-Peng Zhang designed the research. Yun Li performed syntheses and most measurements. Jin Huang and Xue-Wen Zhang measured thermogravimetry and PXRD. Zong-Wen Mo measured IR spectra. Xiao-Ning Cheng measured SEM. Li Gong measured AFM. Yun Li, Dong-Dong Zhou and Jie-Peng Zhang analyzed data and wrote the manuscript.

Appendix A. Supplementary data

Supplementary data to this article can be found online at https://doi.org/10.1016/j.scib.2019.05.011.

References

[1] Dong Y, Wu Z, Ren W, et al. Graphene: a promising 2D material for electrochemical energy storage. Sci Bull 2017;62:724–40.
[2] Jiang W, Wang H, Zhang X, et al. Two-dimensional polymeric carbon nitride: structural engineering for optimizing photocatalysis. Sci China Chem 2018;61:1205–13.
[3] Yang Y, Wu B, Wang L, et al. The synthesis of hexagonal boron nitride via chemical vapor deposition. Sci Bull 2017;62:2195–207.
[4] Zhou L, Shao MF, Wei M, et al. Advances in efficient electrocatalysts based on layered double hydroxides and their derivatives. J Energy Chem 2017;26:1094–106.

[5] Cao LY, Wang TT, Wang C. Synthetic strategies for constructing two-dimensional metal–organic layers (MOLs): a tutorial review. Chin J Chem 2018;36:754–64.
[6] Zhao M, Huang Y, Peng Y, et al. Two-dimensional metal–organic framework nanosheets: synthesis and applications. Chem Soc Rev 2018;47:6267–95.
[7] He T, Ni B, Zhang S, et al. Ultrathin 2D zirconium metal–organic framework nanosheets: preparation and application in photocatalysis. Small 2018;14: e1703929.
[8] Xu M, Yang SS, Gu ZY. Two-dimensional metal–organic framework nanosheets: a rapidly growing class of versatile nanomaterials for gas separation, MALDI-TOF matrix and biomimetic applications. Chem Eur J 2018;24:15131–42.
[9] Sakamoto R, Takada K, Pal T, et al. Coordination nanosheets (CONASHs): strategies, structures and functions. Chem Commun 2017;53:5781–801.
[10] Song WJ. Intracellular DNA and microRNA sensing based on metal–organic framework nanosheets with enzyme-free signal amplification. Talanta 2017;170:74–80.
[11] Ding Y, Chen YP, Zhang X, et al. Controlled intercalation and chemical exfoliation of layered metal–organic frameworks using a chemically labile intercalating agent. J Am Chem Soc 2017;139:9136–9.
[12] Au VK, Nakayashiki K, Huang H, et al. Stepwise expansion of layered metal–organic frameworks for non-stochastic exfoliation into porous nanosheets. J Am Chem Soc 2018;141:53–7.
[13] Zhang JP, Liao PQ, Zhou HL, et al. Single-crystal X-ray diffraction studies on structural transformations of porous coordination polymers. Chem Soc Rev 2014;43:5789–847.
[14] Ghosh SK, Zhang JP, Kitagawa S. Reversible topochemical transformation of a soft crystal of a coordination polymer. Angew Chem Int Ed 2007;46:7965–8.
[15] Cliffe MJ, Castillo-Martinez E, Wu Y, et al. Metal–organic nanosheets formed via defect-mediated transformation of a hafnium metal–organic framework. J Am Chem Soc 2017;139:5397–404.
[16] Wen L, Cheng P, Lin W. Solvent-induced single-crystal to single-crystal transformation of a 2D coordination network to a 3D metal–organic framework greatly enhances porosity and hydrogen uptake. Chem Commun 2012;48:2846–8.
[17] Horike S, Shimomura S, Kitagawa S. Soft porous crystals. Nat Chem 2009;1:695–704.
[18] Huang J, Li Y, Huang RK, et al. Electrochemical exfoliation of pillared-layer metal–organic framework to boost the oxygen evolution reaction. Angew Chem Int Ed 2018;57:4632–6.
[19] Xu M, Yuan S, Chen XY, et al. Two-dimensional metal–organic framework nanosheets as an enzyme inhibitor: modulation of the α-chymotrypsin activity. J Am Chem Soc 2017;139:8312–9.

Yun Li is a Ph.D. candidate of Inorganic Chemistry at Sun Yat-Sen University under the supervision of Prof. Jie-Peng Zhang. His research focuses on design, synthesis and application of PCPs/MOFs.

Dong-Dong Zhou received his Ph.D. degree in 2016 under the supervision of Prof. Jie-Peng Zhang at Sun Yat-Sen University, and is now an associate researcher in the same group. His current research interest focuses on design, synthesis and application of PCPs/MOFs.

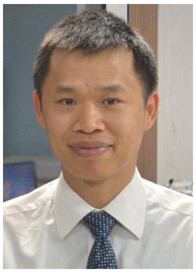

Jie-Peng Zhang obtained his B.Sc degree in 2000 and Ph.D. degree in 2005 at Sun Yat-Sen University (SYSU). He was a JSPS Postdoc at Kyoto University from 2005 to 2007. After that, he moved back and joined SYSU in 2007, and became a professor in 2011. His research focuses on adsorptive separation and electrocatalysis using PCPs/MOFs.